Timing and magma evolution of the Chelopech volcanic complex (Bulgaria)

Schweizerische Mineralogische und Petrographische Mitteilungen 84, 101–117, 2004

Timing and magma evolution of the Chelopech volcanic complex (Bulgaria)

Stanislav Stoykov [1], *Irena Peytcheva* [2,3], *Albrecht von Quadt* [3], *Robert Moritz* [4], *Martin Frank* [3] and *Denis Fontignie* [4]

Abstract

The Chelopech volcanic complex is located in the Central Srednogorie magmatic zone and hosts one of the largest Cu–Au deposits in Europe. Field observations and sedimentary relationships allow to distinguish three units of the volcanic complex: (I) dome-like bodies, (II) lava to agglomerate flows, and (III) the Vozdol lava breccias and volcanites. The volcanic rocks are porphyritic with plagioclase and amphibole phenocrysts, quartz and biotite are rare. The lava flows contain fully crystallised, fine-grained enclaves of more basic composition. Their mineral chemistry indicates mingling and mixing between two parental magmas. The geochemical evolution of the Chelopech volcanic complex developed from intermediate to basic lavas, but the evolution of the magmatism was more complex including magmatic differentiation, assimilation, mingling and mixing. The trace element distribution is typical for an active continental margin.

The magmatic activity commenced at the northern border of the Chelopech region with the intrusion of dome-like bodies at 92.2 ± 0.3 Ma (U–Pb single zircon ID-TIMS dating). The products of the second and the third units are geochronologically indistinguishable within the error uncertainties, and representative samples yield a crystallisation age of 91.3 ± 0.3 Ma. REE abundances reveal a striking positive Ce-anomaly in zircons of unit 2 and zircon core parts of unit 3, which relates to a higher oxidation state of the parental magma.

Sr and Nd isotopic compositions suggest a mixed mantle and crustal source of the Turonian magma. Initial Sr ratios range between 0.70470 and 0.70554, and ε^{90}(Nd) varies between –2.27 and –3.55. ε^{90}(Hf) values of concordant zircons corroborate this data and range between +2.90 to +5.02 in the andesite of the first unit and from +1.06 to +1.38 in the volcanites of the second and third unit.

Keywords: Late Cretaceous volcanites, Chelopech, petrology, U–Pb zircon geochronology, geochemistry.

Introduction

High-sulphidation epithermal deposits are an important gold resource in Eastern Europe, notably in the Bulgarian Panagyurishte region (Central Srednogorie zone, Fig. 1). High-sulphidation, volcanic-hosted, epithermal deposits of economic importance, such as the Chelopech major gold-copper mine (Strashimirov et al., 2002; Moritz et al., 2003), occur in this region. The genesis of the Chelopech mine, the major ore producing epithermal deposit in this area, is related to intermediate Late Cretaceous volcanism, which extruded in the northern part of the Central Srednogorie magmatic zone (Fig. 1). The ideas about the evolution of the magmatic complex changed through time, and one (Terziev, 1968 and recently Jelev et al., 2003), or two (Mutafchiev, 1967; Popov and Mutafchiev, 1980) to four stages of magmatic activity (Popov and Kovachev, 1996) were supposed. Consequently the genetic models for the formation of the Chelopech deposit in relation to the volcanic products evolved, assuming one (the "Chelopech volcano") or two volcanic structures ("Chelopech" and "Vozdol volcanoes"), require one or two mineralising systems respectively. For the timing of the magmatic activity and the mineralisation /alteration products just K–Ar data are available (Lilov and Chipchakova, 1999), which range from 92 to 57 Ma; respectively. The magmatism in the Chelopech region was supposed to be prolonged, but mainly Senonian in age.

The aim of our investigation is to reconstruct the geological evolution of the Late Cretaceous Chelopech volcanic complex and to identify the temporal relationships between its magmatic

[1] University of Mining and Geology 'St. Ivan Rilski', Department of Economic Geology, Studentski grad, Sofia 1700, Bulgaria. <sstoykov@mgu.bg>
[2] Central Laboratory of Mineralogy and Crystallography, Bulgarian Academy of Sciences, Sofia 1113, Bulgaria.
[3] Institute of Isotope Geology and Mineral Resources, ETH-Zentrum, CH-8092 Zürich, Switzerland.
[4] Institute of Earth Sciences, University of Geneva, CH-1205 Geneva, Switzerland.

0036-7699/04/0084/101

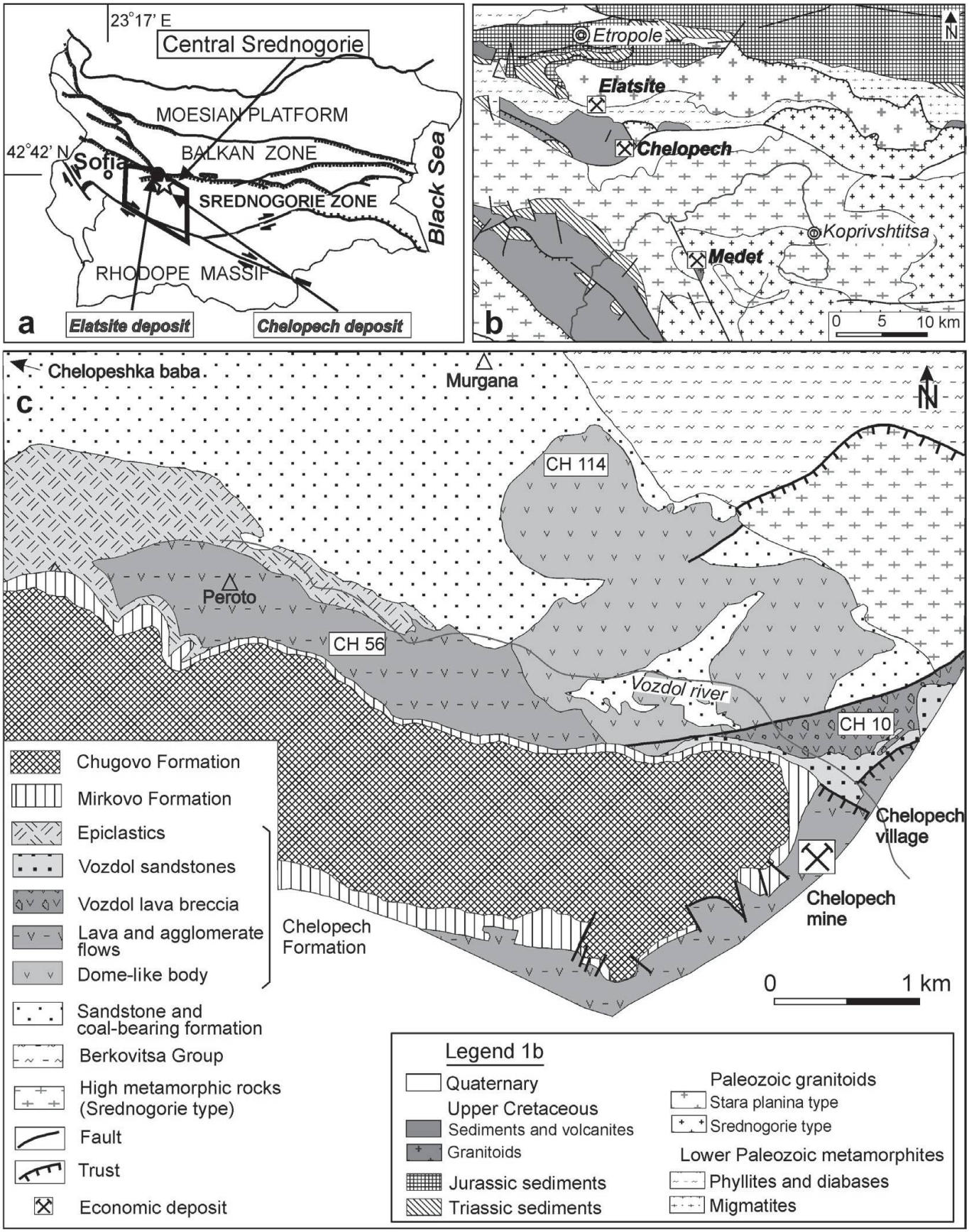

Fig. 1 (a) Major tectonic zones in Bulgaria (after Ivanov, in press) with the location of the Srednogorie zone and Chelopech deposit; (b) Simplified geological map of the northern part of Central Srednogorie (modified after Cheshitev et al., 1989) with the location of the economically important deposits Elatsite, Chelopech and Medet); (c) Geological map of the Chelopech region (modified after Popov et al., 2000 and Stoykov et al., 2002).

products and the mineralised zones outside of the Chelopech mine. An important part of the present study is to trace the magmatic source, determine the precise age of volcanic units, and reconstruct the magmatic processes that may contribute to the formation of the high-sulphidation epithermal Chelopech deposit. We have combined field observations with representative whole rock and mineral geochemical analyses. Conventional U–Pb single zircon dating has been utilised to determine the magmatic ages, as this method combines the relative resistance of the zircons to hydrothermal overprint with the high precision of the ID-TIMS (isotope dilution – thermal ionisation mass spectrometry) techniques. Cathode-luminescence (CL) images and Laser Ablation (LA) ICP-MS analyses of the zircons help the proper interpretation of the geochronological data and give evidence for changes in the geochemistry and oxidation state of the magma. Isotope Sm–Nd and Rb–Sr whole rock and Hf-zircon analyses provide additional information about the magma sources and their evolution.

Geological setting and petrology of the Chelopech volcanic complex

The products of the Chelopech volcanic complex are located in the Central Srednogorie volcano-plutonic area, which forms part of the Srednogorie tectonic zone (Dabovski et al., 1991; Fig. 1). The basement of the volcanic rocks consists of Srednogorie type (Ivanov, in press) high-grade metamorphic rocks (two-mica migmatites with thin intercalations of amphibolites, amphibole-biotite and biotite gneisses), and low metamorphic phyllites and diabases of the Berkovitsa group (Early Paleozoic island-arc volcanic complex, Haydoutov, 2001; Peytcheva and von Quadt, 2004). These units are in tectonic contact with each other, and to the North of Chelopech the phyllites of the Berkovitsa group are intruded by the Variscan granitoids (Kamenov et al., 2002) of the Vejen pluton. The base of the Chelopech volcanic rocks is partly exposed on the surface, although it has been intersected in the underground mine.

The Late Cretaceous succession in the Chelopech region starts with conglomerates and coarse-grained sandstones intercalated with coal-bearing interbeds (coal-bearing formation, Moev and Antonov, 1978) covered by polymictic, argilleous and arkose sandstones to siltstones (sandstone formation). Collectively, these units have a thickness of less than 500 m. Pollen data suggests that both formations are Turonian (Stoykov and Pavlishina, 2003), where the age of 93.5 Ma was taken as transitional from the Cenomanian to the Turonian according to the Geological time scale of the Geological Society of America (Palmer and Geissman, 1999). The sedimentary rocks are cut by volcanic bodies and overlain by sedimentary and volcanic rocks of the Chelopech Formation (Moev and Antonov, 1978). It comprises the products of the Chelopech volcanic complex, epiclastics, as well as the Vozdol sandstones (Fig. 1c). The latter are recently paleontologically dated as Turonian in age (Stoykov and Pavlishina, 2003). These formations have been eroded and transgressively covered by sedimentary rocks of the Upper Senonian Mirkovo Formation (reddish limestones and marls), which are in turn overlain by flysch of the Chugovo Formation (Campanian-Maetrichtian in age, Moev and Antonov, 1978) (Fig. 1b, c).

Based on their structures, host rocks, cross-cutting relationships and alterations on the surface the products of the Chelopech volcanic complex can be subdivided into 3 units: (I) dome-like volcanic bodies, (II) lava and agglomerate flows and (III) the Vozdol volcanic breccias and volcanics (Stoykov et al., 2002, 2003).

The first unit is composed of *dome-like volcanic bodies*, which extruded through the unconsolidated Turonian sediments (the sandstone and coal-bearing formation) and through the metamorphic basement (Fig. 1c). The largest volcanic body (Murgana) is approximately 2×1 km in size. It shows a higher stage of phenocryst crystallisation than the other units. Brecciated fragments of the dome-like volcanic bodies have been observed as xenoliths in the third unit of the Chelopech volcanic complex – the Vozdol volcanic breccia.

The dome-like bodies mainly have an andesitic and trachydacitic composition (Fig. 2). They are highly porphyritic (phenocrysts >40 vol%). The phenocrysts consist of plagioclase, zoned amphibole, minor biotite, titanite and rare corroded quartz crystals, whereas the microlites consist of plagioclase and amphibole only. The accessory minerals are apatite, zircon, and Ti-magnetite. Lilov and Chipchakova (1999) obtained an age of 65–67 Ma for these bodies based on K–Ar dating.

The second unit is represented by *lava flows*, which grade upwards into agglomerate flows (with fragments up to approximately 30 cm in size). Borehole data sho ws that the total thickness of these volcanic products is generally less than 1200 m, but exceeds more than 2000 m in the region of the Chelopech mine ("within their extrusive center", Popov et al., 2002). The composition of the lava flows varies from latitic-trachydacitic to dacitic (Fig. 2). Subsidiary andesites are also present. These volcanic rocks consist of the same phenocrysts, microlites and accessory min-

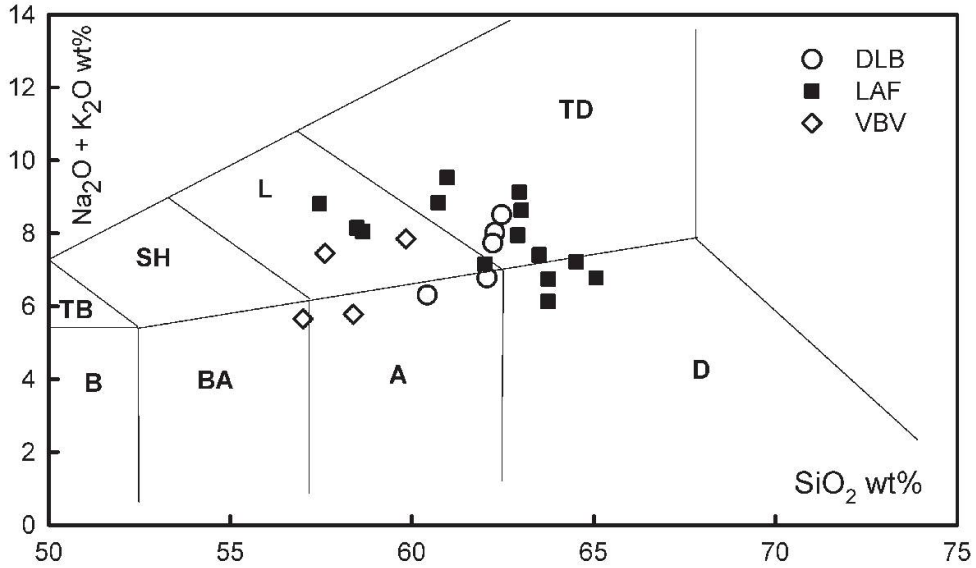

Fig. 2 TAS diagram after Le Maitre (1989) for representative magmatic rocks from the studied region (B—basalt; BA—basaltic andesite; A—andesite; D—dacite; SH—shoshonite; L—latite; TD—trachydacite). DLB—dome-like bodies (unit 1), LAF—lava and agglomerate flows (unit 2), VBV—Vozdol breccias and volcanites (unit 3).

erals as the first unit, with the exception of the corroded quartz crystals. The lava flows contain fine-grained, fully crystallised enclaves of basaltic andesites to shoshonites. The enclaves consist of the same minerals as the main mass of unit 2 (plagioclase, amphibole and minor biotite), but comprise phenocrysts of different (more basic) chemistry. A fine-grained quartz zone marks the margins of the enclaves. These features are typical for magma mingling and mixing processes and are mostly exhibited in the lava flows compared to the other volcanic units. Previous K–Ar dating of non-altered andesite yielded a Turonian age of 91 Ma (Lilov and Chipchakova, 1999).

The third unit is represented by *volcanic breccias and volcanites* that formed the so called Vozdol monovolcano of Popov et al. (2000, 2002). The volcanic breccias contain fragments within their lava matrix that vary in size between 20 and 80 cm. Brecciated fragments from the andesites of the first unit can be observed in outcrops in the Vozdol river valley. The matrix of the volcanic body in the eastern part hosts small lenses and layers of sedimentary material (Vozdol sandstones), and the abundance increases towards the margins of the body. The Vozdol volcanic breccias additionally intercalate and are covered by the Vozdol sandstones (Fig. 1c). The latter has paleontologically been dated as Turonian in age (Stoykov and Pavlishina, 2003). These features may suggest that the extrusion of the third unit volcanites occurred contemporaneous with sedimentation processes in the Turonian. Based on the borehole data and observation in the eastern part of the Chelopech mine, which is not in exploration at present, Popov and Kovachev (1996) and Popov et al. (2000) conclude that the Vozdol volcanic breccias and volcanites form the final stage of the magmatic activity in the Chelopech region, cutting all older products of the volcanic complex, as well as the ore bodies of the Chelopech mine (Popov et al., 2000). On the surface, where our work was concentrated, these relationships are not clear. In the breccias we can observe strongly hydrothermally altered volcanic xenoliths with an obliterated primary texture, which inhibited us to recognise, which type was the initial volcanic rock. Additionally there are detailed studies missing on the alteration type in these xenoliths; the latter are crucial to clarify, if the high-sulfidation type alteration (leading to the deposition of the gold) was genetically linked to the widespread hydrothermal alteration along the Petrovden fault (Fig. 1c, Popov et al., 2000, Jelev et al., 2003), exposed in the Vozdol river valley. Hence we can not conclude about the possible relation of the observed xenoliths to the economic mineralisation (as it was supposed by Jelev et al, 2003).

The composition of the Vozdol volcanites varies from basaltic andesites and andesites to latites (Fig. 2). They show similar petrographic characteristics to the older units although their phenocrysts (plagioclase, amphibole, minor biotite, and titanite) are less abundant. The groundmass is composed of microlites of the same nature as minerals of the second unit. K-feldspar is present as microlites only in the Vozdol andesitic rocks. A biotite $^{40}Ar/^{39}Ar$ age yields a Turonian age of 89.95 ± 0.90 Ma (Velichkova et al., 2001; Handler et al., 2004). Therefore, the K–Ar age of 65 Ma obtained by Lilov and Chipchakova (1999) from samples at the same locality reflects a low-temperature overprint.

Table 1 Major and trace element composition of representative samples of the Chelopech volcanic complex. DLB—dome like bodies (unit 1); LAF—lava and agglomerate flows (unit 2); VBV—Vozdol breccias and volcanites (unit 3).

unit	DLB	DLB	LAF	LAF	VBV
sample No	Ch 113	Ch 121	Ch 37	Ch 56	Ch 10
SiO_2	61.22	60.57	61.07	63.01	57.11
TiO_2	0.54	0.53	0.49	0.51	0.65
Al_2O_3	17.98	17.87	17.68	16.36	18.35
Fe_2O_3	5.01	5.18	4.56	4.94	7.03
MnO	0.14	0.16	0.13	0.12	0.12
MgO	1.44	1.94	1.49	1.63	1.75
CaO	3.38	4.45	4.9	4.91	4.87
Na_2O	5.32	4.28	4.21	3.39	4.19
K_2O	2.70	2.5	2.95	2.74	3.27
P_2O_5	0.25	0.25	0.22	0.23	0.26
LOI	1.73	2.47	1.54	1.16	1.55
Total	99.71	100.2	99.24	99.00	99.15
Nb	7	8	8	7	6
Zr	121	134	126	98	127
Y	23	24	24	20	18
Sr	1430	904	1013	781	871
Rb	72	74	67	63	46
Th	4	6	3	3	3
Pb	17	18	12	16	15
Ga	18	18	17	19	18
Zn	46	57	90	72	137
Cu	25	15	10	26	35
Ni	3	2	2	2	4
Co	50	21	7	10	13
Cr	10	10	12	14	15
V	96	97	101	127	139
Ba	870	778	732	1441	768
S	12	3	140	113	29
Hf	7	6	6	6	6
Sc	6	8	10	10	9
As	11	8	3	6	3
La	34.4	n. d.	28.3	22.9	21
Ce	66.8	n. d.	60.2	49.3	44.7
Pr	6.65	n. d.	6.7	5.3	5.2
Nd	30.1	n. d.	27.7	24	22.8
Sm	5.6	n. d.	5.4	4.9	4.6
Eu	1.41	n. d.	1.3	1.26	1.27
Gd	3.8	n. d.	3.5	3.3	3
Dy	3.5	n. d.	3.5	3.1	3
Ho	0.67	n. d.	0.73	0.66	0.64
Er	2.1	n. d.	2	1.8	1.7
Tm	0.25	n. d.	0.28	0.26	0.24
Yb	1.7	n. d.	1.7	1.5	1.4
Lu	0.24	n. d.	0.24	0.22	0.18

Total Iron as Fe_2O_3. Major concentrations are expressed in wt% and trace element concentrations in ppm respectively; n. d.—not detected.

Several dykes are exposed to the east of to the Chelopech volcanic complex (outside of the map on Fig. 1c). They strike predominately in an east–west direction and intrude into the Pre-upper Cretaceous metamorphic basement. They do not show cross-cutting relationships to the Chelopech volcanic complex. The largest dyke is more than 7 km in length. These dykes have andesitic, latitic, dacitic and trachydacitic compositions.

The magma of the volcanic complex initially erupted more acidic volcanic rocks. The earlier products (dome-like bodies and lava to agglomerate flows) contain 61–64 wt% SiO_2 whereas the more basic Vozdol breccias and volcanites contained 56–58.0 wt% SiO_2. The cover of the Chelopech volcanic complex is composed of the Vozdol sandstones (in the east), muddy limestones of the Mirkovo Formation (in the center) and sedimentary rocks of the Chelopech formation (in the west, Fig. 1c).

Analytical techniques

Major and trace elements

Major and trace elements were analysed by X-ray fluorescence (XRF) at the University of Lausanne, Switzerland. The rare earth elements (REE) were analysed by ICP-atomic emission spectrometry following the procedure of Voldet (1993). A petrological study has also been performed. Mineral analyses on samples of the different units were carried out at the University of Lausanne on a CAMEBAX SX-50 electron microprobe.

U–Pb zircon analyses

High-precision "conventional" U–Pb zircon analyses on single zircon grains utilised the Finnigan MAT 262 thermal ionisation mass-spectrometer at ETH-Zurich using an ion counter system. Selected zircons were air-abraded to remove marginal zones with lead loss, rinsed several times with distilled water, with acetone in an ultrasonic bath, and washed in warm 4 N nitric acid. All samples were spiked with a ^{235}U–^{205}Pb mixed tracer. Total blanks were less than 0.002 ng for Pb and U. The PBDAT and ISOPLOT programs of Ludwig (1988, 2001) were used for calculating the uncertainties and correlations of U/Pb ratios. All uncertainties are reported at the 2σ level. The decay constants of Steiger and Jaeger (1977) were used for age calculations, and corrections for common Pb were made using the Stacey and Kramers (1975) values.

Lu–Hf isotope analyses

Hf isotope ratios in zircons were measured on a Nu Instruments multiple collector inductively coupled plasma mass spectrometer (MC-ICPMS; David et al., 2001) at the Institute of Isotope Geochemistry and Mineral Resources, ETH-Zurich. Testing determined that the high Zr in the sam-

Table 2 U–Pb zircon isotope data for representative samples of the three units of the Chelopech volcanic complex. CH-114—andesite, unit 1; CH-56—trachydacite, unit 2; CH-10—andesite, unit 3.

N	Size fraction μm	weight in mg	#	U ppm	Pb ppm	$^{206}Pb/^{204}Pb$	$^{206}Pb/^{238}U$	2σ error %	$^{207}Pb/^{235}U$	2σ error %	$^{207}Pb/^{206}Pb$	2σ error %	$^{206}Pb/^{238}U$ apparent ages	$^{207}Pb/^{235}U$ apparent ages	$^{207}Pb/^{206}Pb$ apparent ages	*Rho
	CH-10															
1	-100+75	0.0093	long prism beige abr	128.23	3.11	113.7	0.014250	0.81	0.094328	6.9	0.048008	6.5	91.21	91.53	99.69	0.57
2	-100+75	0.0083	long prism beige abr	216.36	3.68	415.2	0.014260	0.72	0.094566	1.22	0.048095	0.96	91.28	91.75	103.93	0.62
3	-100+75	0.0070	long prism beige abr	217.81	3.63	455.7	0.014214	1.09	0.094106	3.13	0.048017	2.79	90.99	91.32	100.09	0.48
4	-125+100	0.0115	long prism beige abr	169.40	5.79	63.5	0.014123	1.08	0.094852	14.1	0.048709	9.53	90.41	92.01	133.87	0.79
5	-125+100	0.0285	long prism beige abr	1001.2	17.35	333.9	0.014291	0.71	0.095494	2.21	0.048465	1.98	91.47	92.61	122.02	0.47
6	-125+100	0.0222	long prism beige abr	147.78	4.49	89.6	0.015881	1.22	0.112706	7.62	0.051471	7.11	101.57	108.44	261.99	0.48
7	-125+100	0.0246	short prism beige abr	171.73	3.08	282.0	0.014327	0.61	0.095727	1.55	0.048459	1.36	91.70	92.82	121.74	0.49
	CH-56															
8	-100+75	0.0146	long prism beige abr	189.42	3.01	597.9	0.014199	1.87	0.094114	2.11	0.048072	0.94	90.89	91.33	102.83	0.90
9	-100+75	0.0065	long prism beige abr	198.12	3.28	433.4	0.014310	0.77	0.096242	1.33	0.048778	1.03	91.59	93.30	137.17	0.63
10	-100+75	0.0106	long prism beige abr 2**	212.91	8.42	52.59	0.013845	1.2	0.091319	7.5	0.047836	6.6	88.64	88.73	91.18	0.85
11	-100+75	0.0122	long prism beige abr 3	188.53	5.36	91.93	0.015275	0.64	0.112006	4.63	0.053180	4.33	97.73	107.80	336.48	0.53
12	-100+75	0.0092	long prism beige abr 2	160.28	2.49	634.5	0.014200	0.59	0.093428	2.59	0.047717	2.4	90.89	90.69	85.27	0.43
13	-100+75	0.0181	long prism beige abr 3	87.12	1.73	768.2	0.017860	0.49	0.122226	0.75	0.049636	0.54	114.11	117.09	177.97	0.69
14	-100+63	0.0313	long prism beige	148.8	2.49	742.1	0.015317	1.30	0.103620	1.60	0.049063	0.96	97.90	100.10	150.80	0.81
15	-100+63	0.0084	long prism beige	122.1	2.16	255.8	0.014068	0.89	0.091831	5.40	0.047342	5.1	90.10	89.20	66.50	0.52
16	-100+63	0.0066	long prism beige	68.77	1.28	243.1	0.014476	0.52	0.122466	1.90	0.061358	1.8	92.60	117.30	651.80	0.50
	CH-114															
17	-125+100	0.0127	long prism beige abr	396.94	14.35	689.2	0.033740	0.61	0.250102	1.27	0.053761	1.06	213.91	226.66	361.07	0.56
18	-125+100	0.0125	long prism beige abr	148.12	3.41	381.05	0.019386	0.63	0.132498	2.54	0.049569	2.34	123.78	126.34	174.83	0.43
19	-100+75	0.0070	long prism beige	383.17	6.23	657.3	0.013943	0.48	0.092401	0.71	0.048064	0.50	89.26	89.73	102.44	0.71
20	-100+75	0.0043	long prism beige	262.12	6.86	879.2	0.024497	0.48	0.176714	0.97	0.052319	0.80	156.02	165.23	299.37	0.57
21	-100+75	0.0034	long prism beige	20.98	0.425	170.4	0.014184	0.56	0.094493	1.14	0.048316	0.95	90.80	91.68	114.78	0.56
22	-100+75	0.0038	long prism beige abr	57.89	1.08	245.9	0.014340	0.56	0.094846	3.17	0.047972	2.97	91.78	92.01	97.87	0.43
23	-100+63	0.0190	long prism limpid abr 5	81.77	1.60	815.8	0.017528	0.57	0.121842	0.89	0.050416	0.66	112.01	116.74	21402	0.67
24	-100+63	0.0195	prism limpid abr 3	146.54	2.34	1606.9	0.015464	0.46	0.104067	0.56	0.048806	0.30	98.93	100.52	138.55	0.84
25	-100+63	0.0226	prism limpid 3	78.72	1.28	728.2	0.014485	0.54	0.096361	1.64	0.048247	1.49	92.71	93.41	111.4	0.44
26	-100+63	0.0160	prism limpid 3	148.63	3.00	201.9	0.014409	0.54	0.095581	2.232	0.048107	2.18	92.23	92.69	104.56	0.37

#: abr — abraded, prism — prismatic; 2** — number of the zircon grains; *Rho — correlation coefficient $^{206}Pb/^{238}U$ – $^{207}Pb/^{235}U$

ples did not create significant matrix effects. During analysis, we obtained a $^{176}Hf/^{177}Hf$ ratio for the JMC 475 standard of 0.282141 ± 5 (1 sigma) using a $^{179}Hf/^{177}Hf$=0.7325 ratio for normalisation (exponential law for mass correction). For the calculation of the ε_{Hf} values the present-day ratios of $(^{176}Hf/^{177}Hf)_{CH}$=0.28286 and $(^{176}Lu/^{177}Hf)_{CH}$=0.0334 were used. For recalculation to 90 Ma a $^{176}Lu/^{177}Hf$ ratio of 0.0050 was taken into account for all zircons.

Rb–Sr and Sm–Nd whole rock isotope analyses

The isotopic composition of Sr and Nd and the determination of Rb, Sr, Sm and Nd contents were performed at ETH-Zurich and the University of Geneva using ID-TIMS techniques. Nd isotopic ratios were normalised to $^{146}Nd/^{144}Nd$= 0.7219. Analytical reproducibility was estimated by periodically measuring the La Jolla standard (Nd) as well as the NBS 987 (Sr). The mean of 12 runs during this work was $^{143}Nd/^{144}Nd$ = 0.511841 ± 0.000007 and 10 runs of the NBS 987 standard show an $^{87}Sr/^{86}Sr$ ratio of 0.710235 ± 0.000006. For further details the reader is referred to von Quadt (1997).

Cathodoluminescence (CL) imaging

The CL-pictures were taken from a split screen on a CamScan CS 4 scanning electron microscope (SEM) at ETH Zurich. The SEM is equipped with an ellipsoidal mirror located close to the sample within the vacuum chamber and can be adjusted by electro-motors. The sample can be located in one focal point while the second focal point lies outside the sample chamber. Here, the CL light enters the highly sensitive photo multiplier through a quartz glass-vacuum window and a light channel. The signal of the photo multiplier is then used to produce the CL picture via a video-amplifier. In general, weak CL emission (dark colours in the picture) means high amounts of minor and trace elements; strong CL emission (light colours in the picture) means low amounts of minor and trace elements.

Laser ablation ICPMS (LA-ICPMS)

Laser ablation ICP-MS spot analyses were done using an Excimer laser (ArF 193 nm) with a gas mixture containing 5% fluorine in Ar with small amounts of He and Ne, connected to a PE SCIEX Elan 6000 ICP-MS. The sample is placed in a closed cell together with the standard material (NIST 612), from which the ablated material is carried out into the ICP-MS by the argon gas stream. We used a spot diameter of 40 µm. The laser pulse repetition rate is 10 Hz. The elements have been detected with 10 ms dwell time and 3 ms quadrupole settling time. The measurement efficiency was around 70%. Backgrounds were measured for 30 s and the transient signals from the sample material to be analysed were acquired for approx. 30 s. Calibrations for the zircon analyses were carried out using NIST 612 glass as an external standard. Limits of detection are calculated as 3 times the standard deviation of the background normalised to the volume of the sample ablated (cps/µg/g). The reproducibility of the data during this work was estimated measuring the NIST 612 standard. For further details we refer to Günter et al. (2001).

Mineral chemistry

The composition of plagioclase phenocrysts of the Murgana dome-like body vary from $An_{38.5–42.2}$ (core) to $An_{38.7–46.2}$ (rim) and those of the lava flows vary from $An_{42.5–48.2}$ (core) to $An_{30.1–53.9}$ (rim). Phenocrysts of the Vozdol breccias and volcanites range between $An_{50.8}$ in the center to $An_{36.2}$ in the periphery. The rims are variable in composition, which substantially overlaps with

Table 3 Hf isotope data for zircons of the Chelopech volcanic complex (numbers as in Table 2).

No	$^{176}Hf/^{177}Hf$*	2σ error	ε-Hf	ε-Hf $T_{90\ Ma}$**
	CH-10			
1	0.282759	0.000006	–0.46	1.03
3	0.282764	0.000003	–0.28	1.20
4	0.282769	0.000003	–0.11	1.38
5	0.282760	0.000002	–0.42	1.06
6	0.282752	0.000002	–0.71	0.78
	CH-56			
8	0.282769	0.000001	–0.11	1.38
9	0.282761	0.000005	–0.39	1.10
10	0.282767	0.000004	–0.18	1.31
11	0.282749	0.000004	–0.81	0.67
12	0.282760	0.000004	–0.42	1.06
	CH-114			
17	0.282761	0.000003	–0.39	1.10
18	0.282807	0.000007	1.24	2.72
19	0.282812	0.000007	1.41	2.90
20	0.282855	0.000012	2.94	4.42
21	0.282872	0.000010	3.54	5.02

* During analysis the $^{176}Hf/^{177}Hf$ ratio (JMC 475 standard) of 0.282141 ± 5 (1σ) using the $^{179}Hf/^{177}Hf$ = 0.7325 ratio for normalisation is measured.

** For the calculation of the ε-Hf values the present-day ratios $(^{176}Hf/^{177}Hf)_{CH}$= 0.28286 and $(^{176}Lu/^{177}Hf)_{CH}$= 0.0334 are used, and for 90 Ma a $^{176}Lu/^{177}Hf$ ratio of 0.0050 for all zircons was taken into account.

that of the phenocryst cores. The composition of plagioclase microlites varies from An_{48} to An_{31}. K-feldspar microlites (Or_{86-93}) were only observed in the Vozdol volcanic breccia and volcanites. Amphiboles from all the volcanic rocks display Mg# between 0.48 and 0.67 and their Si per formula unit content ranges between 6.40 and 6.55. The amphiboles plot on the limit of the magnesio-hastingsite, pargasite, ferropargasite, hastingsite and Fe-edenite field of Leake et al. (1997). The composition of the amphibole phenocrysts of the more mafic enclaves differs to those from the host volcanic rocks. They yield higher Mg#, which range between 0.70 and 0.83 and are magnesio-hastingsites. The Si per formula unit of these amphiboles ranges between 5.90 and 6.10 (Stoykov et al., 2002, 2003). The large variations in Mg# of the amphiboles combined with the reverse mineral zonation of the plagioclase phenocrysts reflect processes of magma mixing and mingling that occurred during the evolution of the Chelopech volcanic complex.

Bulk rock trace elements composition

MORB normalised patterns for the magmatic rocks indicate an enrichment of LILE (large ion lithophile elements) and low values for HFSE (High Field Strength Element) (Ce, Zr, P and Hf) with a strong negative Nb anomaly as well as a depletion of the Fe–Mg elements (Table 1, Fig. 3a). The enrichment of LILE relative to Nb is characteristic of crustal contamination. The LREE enrichment ranges from 33 to 105 (Fig. 3b), whereas La_n/Yb_n ratios vary from 10 to 13. Middle and heavy REEs show relatively flat patterns, which are generally within 5–30 times that of chondrite. The rocks from the Murgana dome-like body re-

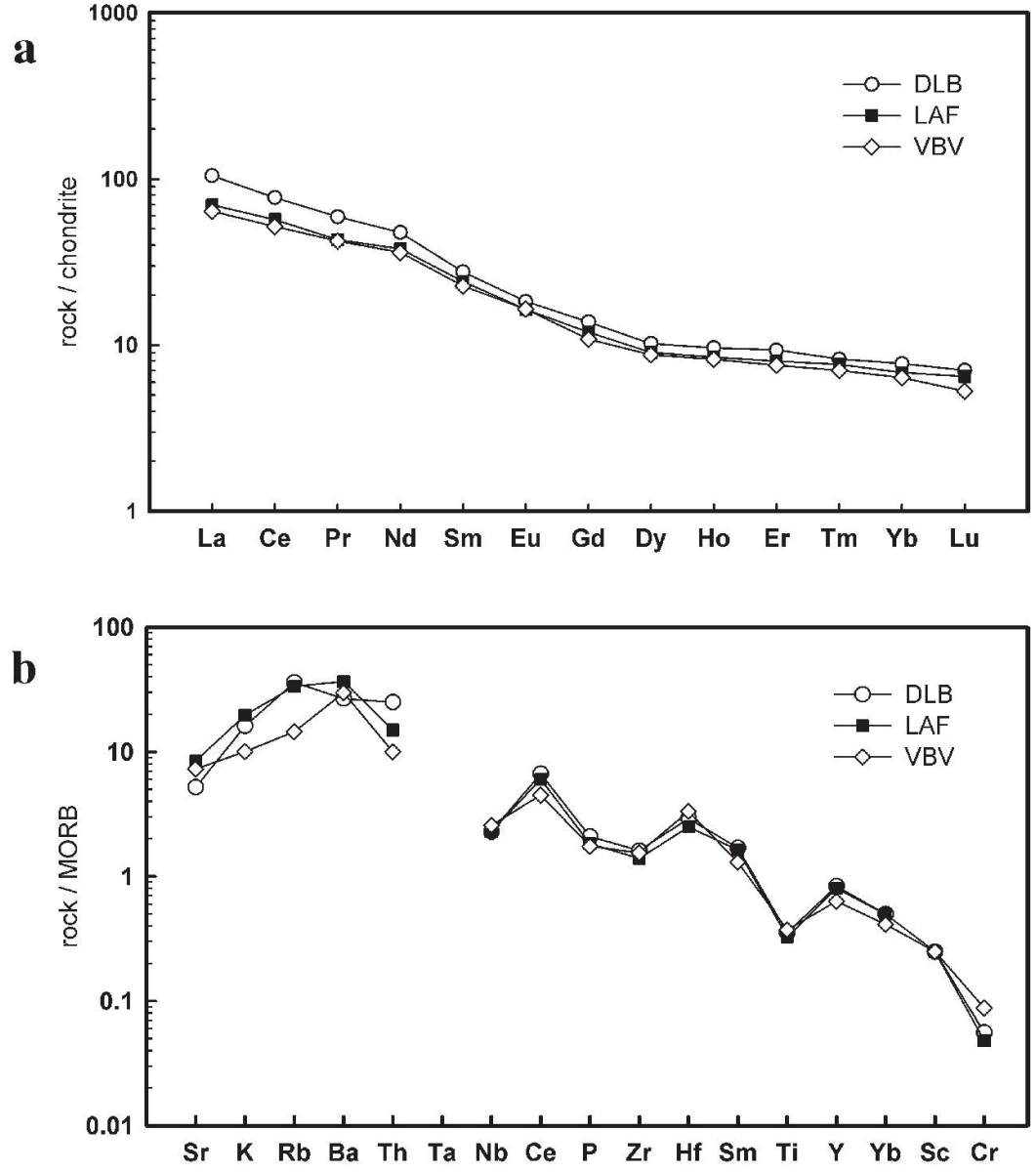

Fig. 3 (a) REE diagram for magmatic rocks of the Chelopech region; (b) spider discrimination plot for the volcanic rocks of the Chelopech volcanic complex. Data symbols as in Fig. 2.

veal slightly enriched values of LREEs compared to the lava flows and the Vozdol volcanic breccia (Fig. 3). An Eu anomaly is not observed, which suggests that there was no plagioclase fractionation involved during the genesis of the andesitic rocks. All these features are typical for subduction-related magmatic sequences. Discrimination diagrams TiO_2/Al_2O_3 vs. Zr/Al_2O_3 and Zr/TiO_2 vs. Ce/P_2O_5 (Müller et al., 1992) show similar composition to active continental margin magmatic products (Fig. 4).

U–Pb zircon geochronology and Hf zircon isotope geochemistry

Zircons were separated from the three different units of the Chelopech volcanic complex (Fig. 1c). Ten zircon grains of an andesite sample CH-114 from the Murgana dome-like body (unit 1) were dated (Table 2). Three of them (22, 25 and 26, long prismatic, beige) are plotting on the concordia within their uncertainties and define a mean $^{206}Pb/^{238}U$ age of 92.22 ± 0.30 Ma (Fig. 5). We interpret that these concordant grains most closely represent the time of intrusion of the andesite body. Two of the zircon grains reveal lead loss, but most of the measured zircons have lead inheritance. The regression line through four corresponding points yields an upper intercept age of 467 ± 28 Ma indicating an Early Paleozoic event (the age of the metamorphic basement?), whereas one of the analyses (No. 8, Table 2) give evidence for a possible Hercynian inheritance (the Variscan granites of the Balkan or of the Srednogorie?). The ε^{90}(Hf) of the zircons range from +1.10 to +5.02 (Table 3). The zircon grain with the highest apparent age (No. 17, Table 2, 3) shows the lowest ε^{90}(Hf) and gives evidence for upper crustal characteristics of the assimilated materials. On the other hand there is no clear correlation between lead inheritance and decrease of the ε^{90}(Hf) values, which is possibly not only due to the fact, that some grains are abraded and others not, but more to source differences and inhomogeneities.

The U–Pb isotope systematic of the zircon fractions of a trachydacite (CH-56, Table 2) from the second unit shows characteristics of lead inheritances and lead losses. Four data points are almost concordant and define a mean $^{206}Pb/^{238}U$ age of 91.3 ± 0.3 Ma (Fig. 6). The ε^{90}(Hf) of the concordant zircons change in a narrow range of +1.06 to +1.38 (Table 3) indicating a mixed crustal and mantle origin of the magma, but more crustal influence, compared to the andesite of the first unit (CH-114, Table 2). The inherited old Pb components for two zircon points (Table 2, No. 13, 14) refer to an upper intercept "Variscan age" of the assimilated crustal material.

Five out of seven zircon analyses of an andesite from the Vozdol lava breccia neck (CH-10, third unit) are concordant (Fig. 7, Table 2) and yield a mean $^{206}Pb/^{238}U$ age of 91.3 ± 0.3 Ma. It coincides within error limits with the age of the lava flow sample of the second unit. Some similar

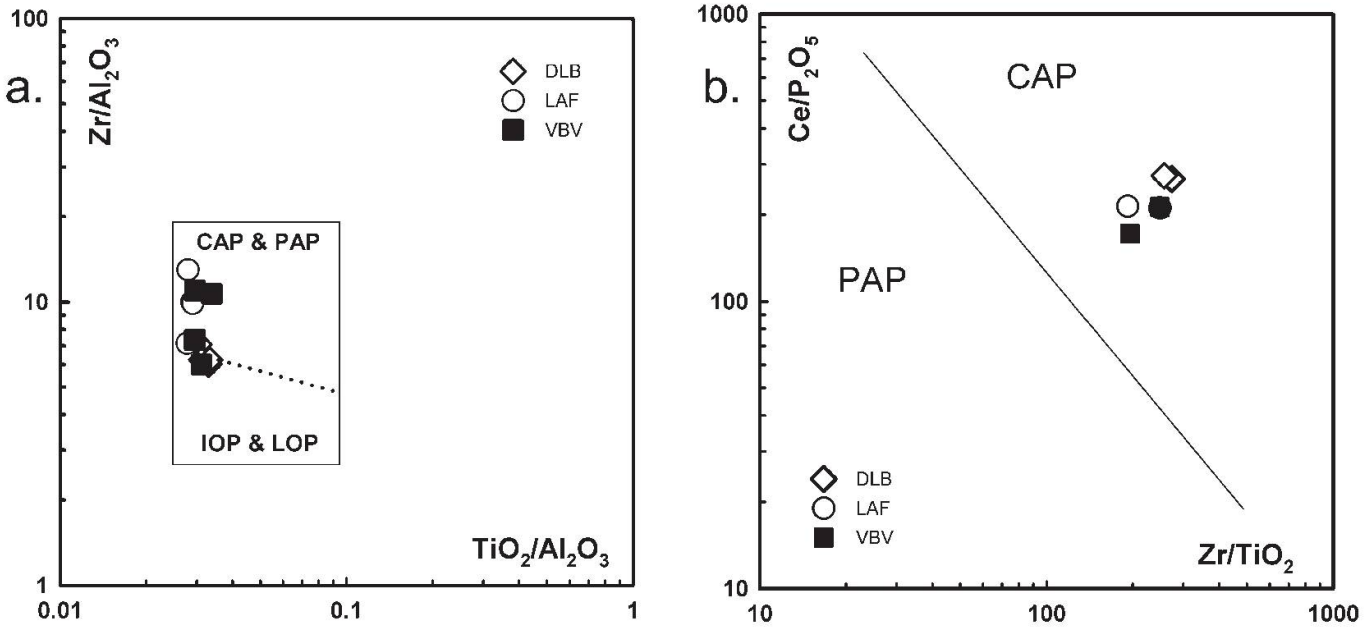

Fig. 4 (a) TiO_2/Al_2O_3 vs. Zr/Al_2O_3 and (b) Zr/TiO_2 vs. Ce/P_2O_5 discrimination diagrams (Müller et al., 1992). CAP—Continental Arc; PAP—Postcollisional Arc; IOP—Initial oceanic Arc; LOP—Late oceanic Arc; WIP—Within-plate. For data symbols see Fig. 2.

features of both samples are revealed by the ε^{90}(Hf) values of the concordant zircons, changing in one and the same narrow range of +1.06 to +1.38 (Table 3, Fig. 7). These similarities with close Hf-isotope characteristics is typical for both volcanic units.

CL-features and REE geochemistry of the zircons

Using cathode-luminescence (CL) images and the Excimer Laser Ablation (LA) ICP-MS analyses (Table 4) we tried to characterise the inner

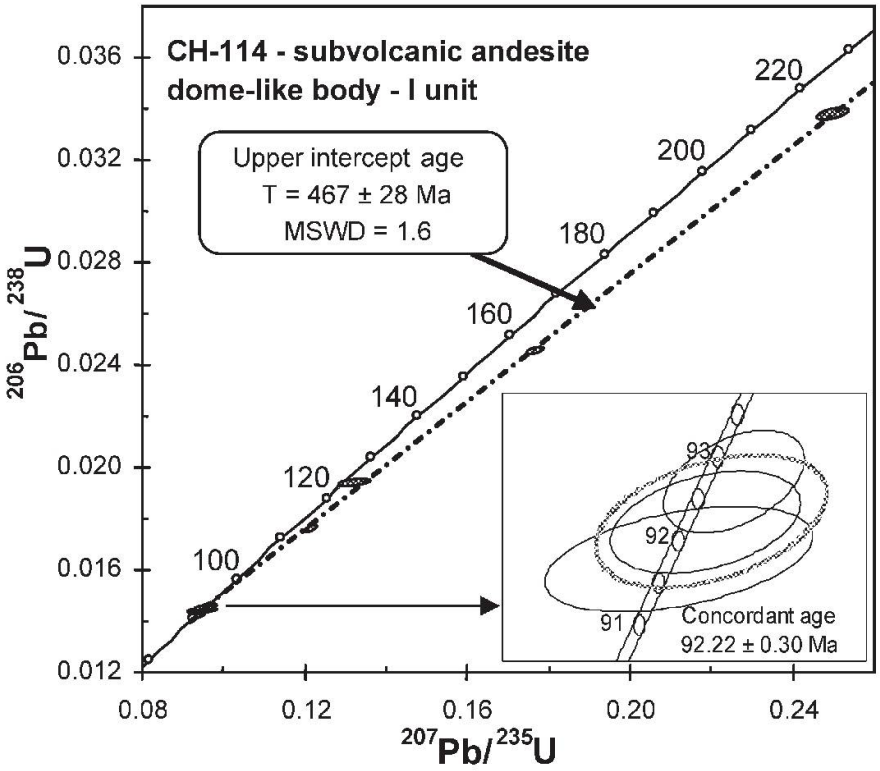

Fig. 5 U–Pb concordia diagram for zircons of an andesite CH-114 (Murgana dome-like body) representing the first unit of the Chelopech volcanic complex.

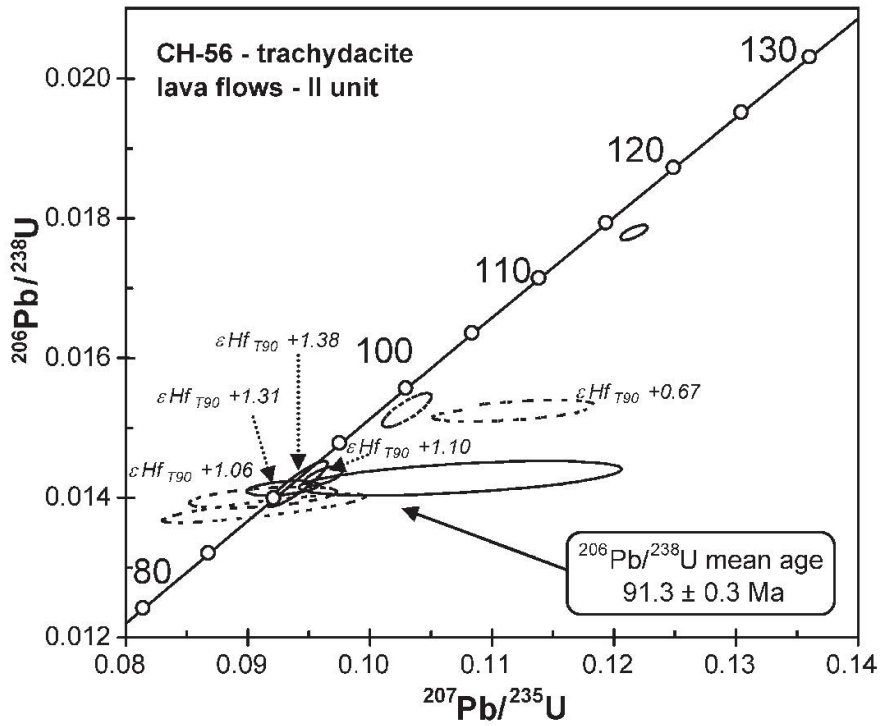

Fig. 6 U–Pb concordia diagram for zircons of trachydacite CH-56, representing the second unit of the Chelopech volcanic complex. Solid error ellipse lines are used for the concordant zircons and dashed error ellipse lines mark zircons with lead loss or lead inheritance. The ε–Hf data of Table 3 are plotted for the corresponding data points.

peculiarities and the chemistry of the zircons from the first to the third unit of the Chelopech volcanic complex, which helps us to control the proper interpretation of the geochronological U–Pb zircon data. This precise study was provoked additionally by recently published data of Ballard et al. (2002) for calc-alkaline intrusions from the porphyry copper belt in Chile, where a high Ce(IV)/Ce(III) ratio was characteristic for the rocks with economic potential, bearing magmatic-hydrothermal Cu ± Au. It is known, that this positive anomaly is related to the higher oxidation state of the parental magma that leads to oxidation of Ce^{3+} to Ce^{4+}; the latter easily substitutes Zr^{4+} in the lattice of zircon (Cornell and Hegardt, 2003). The higher oxidation state of the parental magma from the other side is usually considered as a prerequisite feature of the ore-producing magmatism.

The typical magmatic oscillatory zoning is observed in all zircon images (Fig. 8). The intermediate and heavy rare earth elements (REE) reveal a

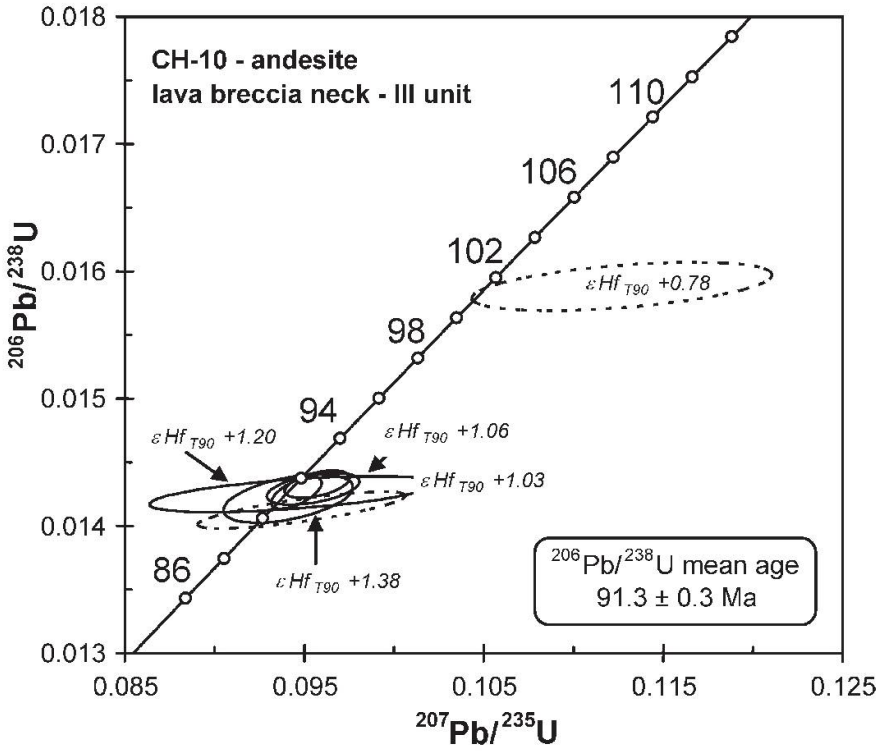

Fig. 7 U–Pb concordia diagram for zircons of the andesite sample CH-10 from the Vozdol lava breccia neck, representing the third unit of the Chelopech volcanic complex. Error ellipse symbols as in Fig. 6. The ε–Hf data of Table 3 are plotted for the corresponding data points.

Table 4 Rare earth element contents (ppm) in zircons of the three units of the Chelopech volcanic complex.

Sample No Element	CH56-C	CH56-R	CH10-C	CH10-R	CH114-C	CH114-R
La	0.149	0.030	0.038	2.176	4.273	0.214
Ce	22.35	19.33	14.13	45.63	15.85	15.51
Pr	0.061	0.037	0.033	0.789	0.998	0.168
Nd	1.027	0.453	0.279	4.752	4.017	1.133
Sm	2.701	1.715	0.589	4.660	1.059	1.210
Eu	1.309	0.800	0.436	2.000	0.330	0.878
Gd	15.99	9.332	5.288	23.17	5.611	9.165
Tb	6.541	3.965	2.019	9.676	2.366	3.365
Dy	84.82	54.35	28.88	134.4	28.84	44.82
Ho	37.13	24.38	14.98	58.76	12.49	20.43
Er	191.4	134.4	88.59	302.2	65.01	114.8
Tm	45.92	35.37	24.40	72.90	16.10	29.59
Yb	523.8	420.7	304.5	799.4	188.2	350.2
Lu	116.3	99.42	80.28	168.4	41.86	82.62

Abbreviations: C—core, R—rim.

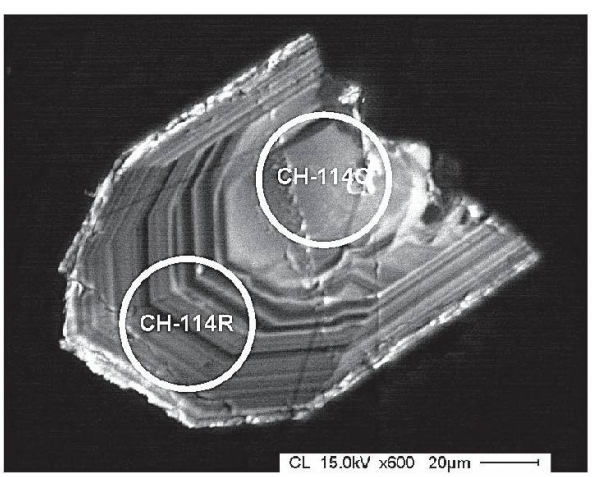

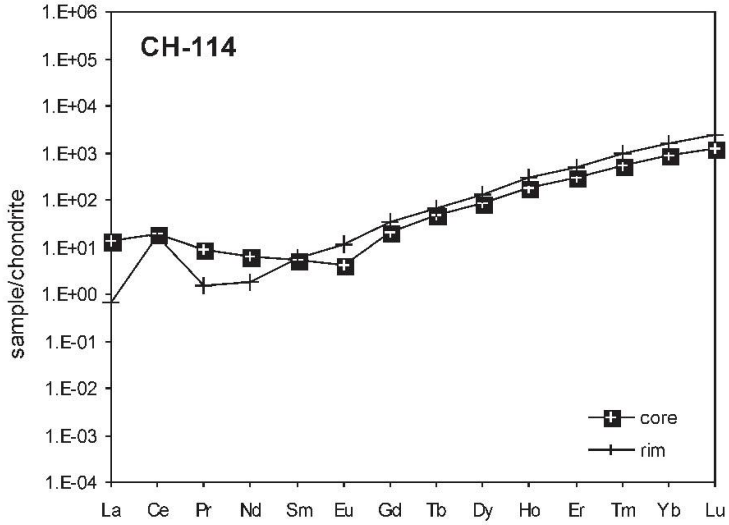

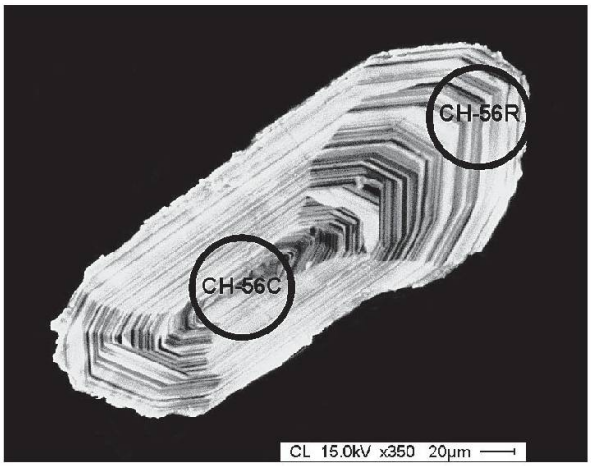

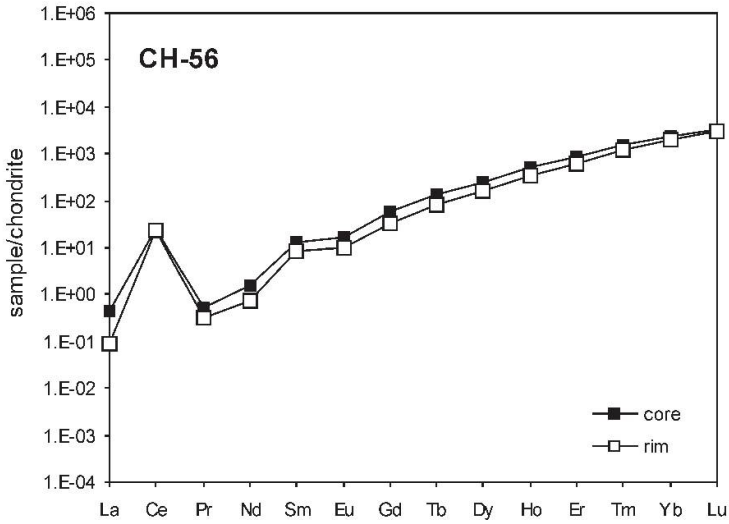

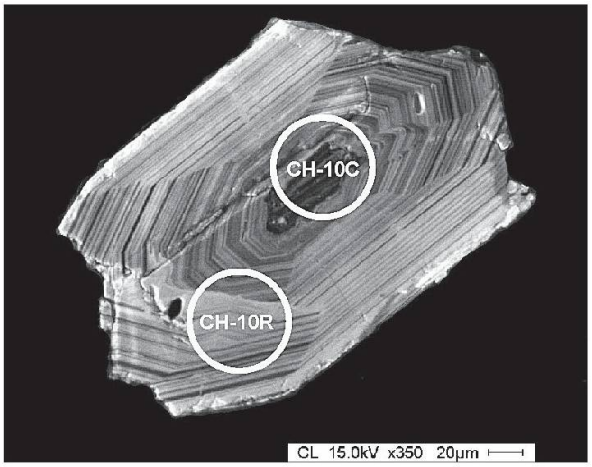

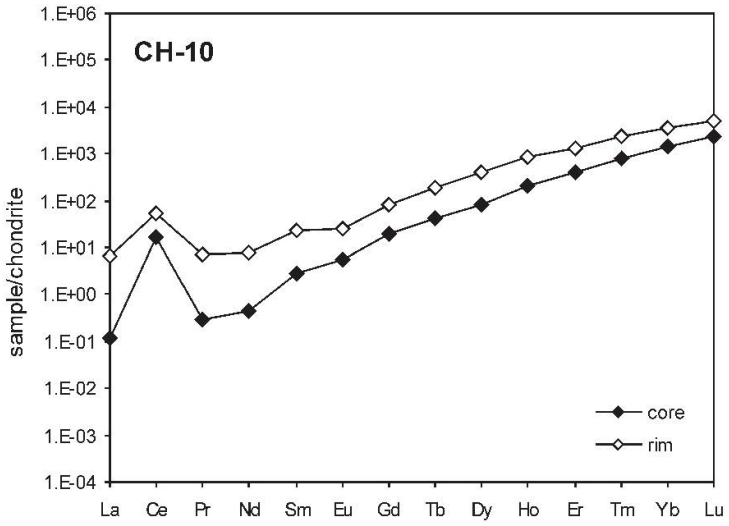

Fig. 8 Cathode-luminescent (CL) images of zircons from the three units of the Chelopech volcanic complex with the corresponding chondrite-normalised distribution of the REE. Circles on the pictures correspond to the laser ablation spot in the zircon crystals.

constant and typical magmatic (Hoskin and Irland, 2000; Belousova et al., 2002) distribution. Eu anomaly is not observed in the zircons, which confirms the conclusion (based on the rock chemistry) that there was no plagioclase fractionation during the genesis of the andesitic magma.

A recrystallised inherited zircon core is observed within the first unit sample CH-114 (Fig.

Table 5 Rb–Sr and Sm–Nd isotope data for whole rock samples of the Chelopech volcanic complex.

Nr	rock type	unit	Rb (ppm)	Sr (ppm)	$^{87}Rb/^{86}Sr$	$^{87}Sr/^{86}Sr$	2σ error	$(^{87}Sr/^{86}Sr)_{i90}$	Sm (ppm)	Nd (ppm)	$^{147}Sm/^{144}Nd$	$^{143}Nd/^{144}Nd$	2σ error	$(^{143}Nd/^{144}Nd)$ T=90	ε-Nd T= 90
56	trachydacite	2	118	905	0.3783	0.705187	0.000022	0.704703	2.41	14.63	0.0992	0.512464	0.000042	0.512406	–2.27
81	andesite	1	99	695	0.4114	0.705750	0.000027	0.705224	3.15	17.01	0.1117	0.512444	0.000013	0.512378	–2.81
114	andesite	1	209	925	0.6539	0.705686	0.000037	0.704850	3.01	15.85	0.1147	0.512445	0.000069	0.512377	–2.82
37i	andesite enclave	2	35	403	0.2534	0.705519	0.000016	0.705195	4.35	20.72	0.1268	0.512425	0.000022	0.512350	–3.35
10	andesite	3	46	871	0.1480	0.705133	0.000007	0.704944	4.60	22.80	0.2018	0.512459	0.000001	0.512340	–3.55
24	latite	1	72	623	0.3230	0.705845	0.000007	0.705432	5.60	39.00	0.1436	0.512457	0.000009	0.512372	–2.92
37	dacite	2	67	1013	0.0660	0.705620	0.000001	0.705536	5.40	27.70	0.1960	0.512460	0.000007	0.512345	–3.46

8), which is in agreement with the U–Pb data, showing inherited lead (Table 2 and Fig. 5). The chondrite-normalised pattern of the REE changes in this core, compared to the outer magmatic zone. The striking features are specially marked in the distribution of the light REE and the Ce positive anomaly. As we already calculated an Early and Late Paleozoic age of the inherited zircon cores we can conclude, that the parental Paleozoic magma either missed the high oxidation and/or Ce was released during later geological processes, e.g. the metamorphism of the basement rocks or the dissolution of the zircons in the Cretaceous magma.

The entire zircon of CH-56 (trachydacite of the second unit), as well as the zircon core part of CH-10 (andesite of the third unit) reveal well-defined Ce positive anomalies, marking therefore higher oxidation state of the magma. The rim part of CH-10 lost the well-pronounced positive Ce anomaly, which possibly means changing of the relative oxidation state of the magma in the time when the zircon still crystallised (possible mixing with a new portion of magma in the chamber?).

Sr and Nd isotope geochemistry and magma sources

The initial Sr isotope ratios of the magmatic rocks from the Chelopech volcanic complex and the dykes show a small range between 0.70470 and 0.70554 at Cretaceous time (90 Ma correction; Table 5). Generally, the initial $^{87}Sr/^{86}Sr$ ratios fall within the field previously defined by Kouzmanov et al. (2001) and von Quadt et al. (2003) in the range 0.7046 to 0.7061 for Late Cretaceous magmatites in Central Srednogorie and show similarities with published initial Sr values of the Apuseni-Banat-Timok-Srednogorie belt (Berza et al., 1998; Dupont et al., 2002; von Quadt et al., 2001, 2003). The calculated ε^{90}(Nd) values are between –2.27 and –3.55. These data together with the ε^{90}(Hf) of the zircons suggest a mixed mantle-crust source of the Turonian magmatism in the Chelopech region.

The $(^{87}Sr/^{86}Sr)_i$ vs. $(^{143}Nd/^{144}Nd)_i$ diagram (Fig. 9) demonstrates that all data points plot close to the enriched mantle type 1 (EM1) field, which is typical for island arc volcanites. Some peculiarities of the bulk rock chemistry and of the zircons give evidence for additional interaction of the enriched mantle source magma with crustal materials. However using the variations of the initial Sr and Nd ratios vs. SiO_2 the evolution of the magma may be largely due to mingling/mixing processes, without isotope homogenisation in the whole vol-

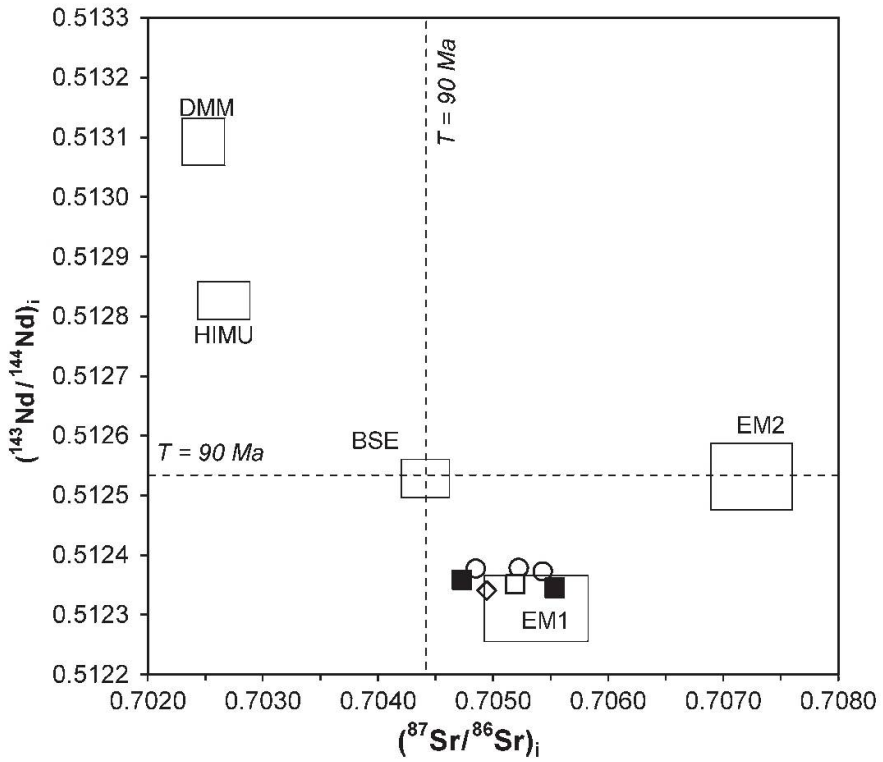

Fig. 9 $(^{87}Sr/^{86}Sr)_i$ vs. $(^{143}Nd/^{144}Nd)_i$ diagram for rock samples of Chelopech volcanic complex. Fields of the DMM (depleted MORB mantle), HIMU (magma source having a high μ-$^{238}U/^{204}Pb$ ratio), EM1 and 2 (enriched mantle 1 and 2) and BSE (bulk silicate earth) are given (corrected for 90 Ma) according to Zindler and Hart (1986) and Hart and Zindler (1989). Dashed lines correspond to the Sr and Nd isotope values of the undifferentiated reservoir – identical to CHUR (DePaolo, 1988; Faure, 2001), corrected for 90 Ma. For data symbols see Fig. 2.

ume of the magma chamber, and not to a simple differentiation of one parental magma, combined or not with assimilation of upper crustal rocks.

Discussion and constraints for timing and magma sources

The high-precision U–Pb zircon data demonstrate that the magmatic activity of the Chelopech region started at the northern border with the intrusion of the dome-like bodies at 92.3 ± 0.5 Ma. The products of the second and the third units followed closely one after the other and they are undistinguishable within their uncertainties: U–Pb analyses of zircons of representative samples yield an intrusion age of 92.22 ± 0.30 Ma. The lava breccias of the third unit contain fragments of the first unit, hence the geological relationships in the field are in agreement with isotope geochronological data. The high-sulphidation epithermal Cu–Au mineralisation is hosted by the volcanites of the second unit. Assuming the error uncertainties we can calculate a maximum age of 91.6 Ma for the epithermal deposit, which coincides with the recently published data of Chambefort et al. (2003) and Moritz et al. (2003). The minimum age of the deposit is still not constrained. As it was mentioned in the above chapters, present investigations are focussed on the special features of the volcanic products on the surface, so that we still are not able to link the strongly altered volcanic xenoliths in the volcanic breccias of the third unit to a distinct mineralising stage.

Chondrite-normalised patterns of REE and trace elements in the zircons (LA ICP-MS analyses) reveal a well-pronounced positive Ce anomaly in the zircon grains of the second unit (trachydacite) and in the zircon core of the third unit (andesite). The latter may be related to a higher oxidation state of the parental magma – a prerequisite feature of an ore-producing magmatism. These data just show the potential of the second unit volcanites to be the fertile phase of the volcanic complex, but are far away to prove this, as the formation of one deposit is a combination of factors, which study was not the aim of the present work.

There is commonly a close spatial relation between porphyry Cu (± Au) and high-sulphidation epithermal Cu–Au deposits through the world and the close temporal relation between them should be an argument for their genetic link (Arribas et al., 1995). The world-class porphyry Cu deposit Elatsite is located about 6 km to the NNW of the Chelopech high-sulphidation epithermal Cu–Au deposit and a genetic link between them was proposed by Popov et al. (2002). The ore-pro-

ducing magmatism in Elatsite was bracketed in the time span 92.1 ± 0.3 Ma to 91.84 ± 0.31 Ma using high-precise U–Pb zircon dating (von Quadt et al., 2002) and confirmed later by Re–Os molybdenite age determinations in the range of 93.1–92.3 Ma (Zimmermann et al., 2003). For a non-productive dyke of the deposit von Quadt et al. (2002) obtained a mean $^{206}Pb/^{238}U$ age of 91.42 ± 0.15. Compared with the present data of the Chelopech volcanic complex there is an overlap between the ore-producing magmatism in Elatsite and the dome-like andesitic bodies. The final barren stage of the magmatism in Elatsite was almost contemporaneous with the volcanic rocks that host the Chelopech deposit. The age data do not discard therefore the model of a common magmatic chamber for both deposits with some pulses of intrusion/extrusion of magmatites. Unfortunately we did not observed the published data about structures between the Chelopech and the Elatsite deposits, which could explain the horizontal distance of about 6 km and the vertical displacement of about 1 km. Therefore present isotope-geochronological data are not enough to favour the idea for one and the same magmatic-hydrothermal system for both deposits.

The petrological and geochemical features give additional evidence for a possible uniform magma chamber of the volcanic rocks in the Chelopech and Elatsite deposits with a complex evolution in Turonian times, when a combination of processes of magmatic differentiation, assimilation, mingling and mixing took place. The magmatic products in Elatsite and Chelopech reveal similar Sr, Nd and Hf characteristics, where the tendency of an increase of ε^{90}(Nd) and a decrease of ε^{90}(Hf) zircon could be related to minor assimilation of host rocks within parts of the magmatic chamber. The amphibole chemistry of the magmatic units of both deposits shows some similar characteristics – Mg# between 0.48 and 0.67 and Si per formula unit content between 6.40 and 6.55, but mark differences comparing to the other deposits of the Panagyurishte ore region (Kamenov et al., 2003).

Conclusions

The combined petrologic, isotope-geochemical and geochronological investigations of the Chelopech volcanic complex suggest:

– The three units of the Chelopech volcanic complex are separated on the basis of their structural, textural, petrographical, and geochemical characteristics including the chemistry of the phenocrysts.

– the magmatic activity proceeded in Turonian time, starting with the intrusion of the dome-like bodies at 92.2 ± 0.3 Ma and finishing with the formation of the Vozdol breccias and volcanites at 91.3 ± 0.3 Ma;

– Nd and Sr whole rock and Hf-zircon characteristics argue for mixed crustal-mantle origin of the magma for all three volcanic units;

– the evolution of the magmatism was defined by processes of magma mingling and mixing, differentiation and assimilation of crustal rocks;

– a maximum age of 91.6 Ma of the Chelopech Cu-Au deposit could be calculated based on the dating of the second unit volcanites, hosting the economic mineralisation; the positive Ce anomaly in zircon from the same unit gives evidence for the high oxidation state of the magma.

– additional studies on the relationships of the volcanic units to the economic mineralisation and altered rocks, as well as detailed tectonic investigations will help to constrain the age of the Chelopech deposit and to create reasonable models of its formation or possible link to adjacent deposits.

Acknowledgements

This work was supported by the Swiss National Science Foundation through the SCOPES Joint Research Projects 7BUPJ062276 and 7BUPJ62396 and research grant 21-59041.99. Present study is a contribution to the ABCD-GEODE (Geodynamics and Ore Deposits Evolution of the Alpine-Balkan-Carpathian-Dinaride Province) research program supported by the European Science Foundation. The authors would like to thank the geological staff of the Chelopech mine for their help during the visits of the deposit. Z. Cherneva and M. Popov are kindly acknowledged for the help in sample preparation and the zircon separation, and P. Voldet (University of Geneva) for REE whole rock data acquisition. R. Spikings is thanked for the corrections of the English. The authors are grateful to the two reviewers W. Halter and J. Lexa and the guest-editors of the special SMPM issue for their constructive suggestions and corrections that helped to improve the manuscript.

References

Arribas, A., Hedenquist, Jr., Itaya, J.W., Okada, T., Concepcion, R.A. and Garcia, J.S. (1995): Contemporaneous formation of adjacent porphyry and epithermal Cu-Au deposits over 300 ka in northern Luzon, Phillippines. *Geology* **23**, 337–340.

Ballard, J.R., Palin, M.J. and Campbell, J.H. (2002): Relative oxidation states of magmas inferred from Ce(IV)/Ce(III) in zircon: application to porphyry copper deposits of Northern Chile. *Contrib. Mineral. Petrol.* **144**, 347–364.

Belousova, E., Griffin, W., O'Reilly, S. and Fisher, N. (2002): Igneous zircon: trace element composition as an indicator of source rock type. *Contrib. Mineral. Petrol.* **143**, 602–622.

Berza, T., Constantinescu, E. and Vlad, S.-E. (1998): Upper Cretaceous magmatic series and associated mineralisation in the Carpathian-Balkan orogen. *Resource Geology* **48/4**, 291–306.

Cheshitev, G., Kanchev, I., Valkov, V., Marinova, R., Shiljafova, J., Russeva, M. and Iliev, K. (1989): Geological map of Bulgaria, scale 1:500000.

Chambefort, I., von Quadt, A. and Moritz, R. (2003): Volcanic environment and geochronology of the Chelopech high-sulfidation epithermal deposit, Bulgaria: regional relationship with associated deposit. *Geoph. Research Abstr.* **5**, 00569 (CD version).

Cornell, D.H. and Hegardt, E.A. (2003): No more blind dates with zircon! *Geoph. Research Abstr.* **5**, 02524 (CD version).

Dabovski, Ch., Harkovska, A., Kamenov, B., Mavrudchiev, B., Stanisheva-Vasileva, G. and Yanev, Y. (1991): A geodynamic model of the Alpine magmatism in Bulgaria. *Geol. Balcanica* **21/4**, 3–15.

Dabovski, C., Boyanov, I., Khrischev, Kh., Nikolov, T., Sapunov, I., Yanev, Y. and Zagorchev. I. (2002): Structure and Alpine evolution of Bulgaria. *Geol. Balcanica* **32/2–4**, 9–15.

David, K., Frank, M., O'Nions, R.K., Belshaw, N.S. and Arden, J.W. (2001): The Hf isotope composition of global seawater and the evolution of Hf isotopes in the deep Pacific Ocean from Fe–Mn crusts. *Chem. Geol.* **178**, 23–42.

DePaolo, D.J. (1988): Neodymium isotope geochemistry. Springer Verlag Berlin, 187 pp.

Dupont, A., Vander Auwera, J., Pin, C., Marincea, S. and Berza, T. (2002): Trace element and isotope (Sr, Nd) geochemistry of porphyry- and scarn-mineralising Late Cretaceous intrusions in Banat, western South Carpathians, Romania. *Mineralium Deposita* **37/6–7**, 568–586.

Faure, G. (2001): Origin of igneous rocks: the isotopic evidence. Springer Verlag Berlin, 496 pp.

Günther, D., von Quadt, A., Wirz, R., Cousin, H. and Dietrich, V. (2001): Elemental analyses using Laser Ablation-Inductively Coupled Plasma-Mass Spectrometry (LA-ICP-MS) of Geological samples fused with $Li_2B_4O_7$ and calibrated without matrix-matched standards. *Mikrochimica Acta* **136**, 101–107.

Handler, R., Neubauer, F., Velichkova, S. and Ivanov., Z. (2004): $^{40}Ar/^{39}Ar$ age constraints on the timing of magmatism and post-magmatic cooling in the Panagyurishte region, Bulgaria. *Schweiz. Mineral. Petrogr. Mitt.* **84,** 119–132.

Hart, S.R. and Zindler, A. (1989): Constraints on the nature and development of chemical heterogeneities in the mantle. In: Peltier, W.R. (ed.): Mantle convection. Gordon and Breach Science Publishers, New York, 261–382.

Haydoutov, I. (2001): The Balkan island-arc association in West Bulgaria. *Geol. Balcanica* **31/1–2**, 109–110.

Hoskin, P. and Irland, T. (2000): Rare earth chemistry of zircon and its use as a provenance indicator. *Geology* **28/7**, 627–630.

Ivanov, Z. (2002): Tectonics of Bulgaria. (in press)

Kouzmanov, K., Moritz, R., Chiaradia, M. and Ramboz, C. (2001): Sr and Pb isotope study of Au–Cu epithermal and porphyry-Cu deposits from the southern part of the Panagyurishte district, Sredna Gora zone, Bulgaria. In: Piestrzynski et al. (eds.): Mineral Deposits at the Beginning of the 21st Century. Swets & Zeitlinger Publishers, Lisse, 539–542.

Kamenov, B., von Quadt, A. and Peytcheva, I. (2002): New insight into petrology, geochemistry and dating of the Vejen pluton, Bulgaria. *Geochem. Mineral. Petrol.* **39**, 3–25.

Kamenov, B. K., Nedialkov, R., Yanev, Y. and Stoykov, S. (2003): Petrology of Late Cretaceous ore-magmatic centers from Central Srednogorie, Bulgaria. In: Bogdanov, K. and Strashimirov, S. (eds.): Cretaceous porphyry-epithermal systems of the Srednogorie zone, Bulgaria. *Society of Economic Geologists. Guidebook Series* **36**, 133 pp.

Leake, B.E., Woolley, A.R., Arps, C.E.S., Birch, W.D., Gilbert, M.C., Grice, J.D., Hawthorne, F.C., Kato, A., Kisch, H.J., Krivovichev, V.G., Linthout, K., Laird, J., Mandariano, J., Maresch, W.V., Nickel, E.H., Rock, N.M.S., Schumacher, J.C., Smith, D.C., Stephenson, N.C.N., Ungaretti, L., Whittaker, E.J.W. and Youzhi, G. (1997): Nomenclature of amphiboles. Report of the Subcommittee on amphiboles in the IMAC on new minerals and minerals names. *Eur. J. Mineral.* **9**, 623–651.

Le Maitre, R.W. (1989): A Classification of igneous rocks and glossary of terms. Oxford, Blackwell Sci. Publ., 193 pp.

Lilov, P. and Chipchakova, S. (1999): K–Ar dating of the Late Cretaceous magmatic rocks and hydrothermal metasomatic rocks from Central Srednogorie. *Geochem. Mineral. Petrol. Sofia* **36**, 77–91 (in Bulgarian with English abstract).

Ludwig, K.R. (1988): PBDAT for MS-DOS; a computer program for IBM-PC compatibles for processing raw Pb–U–Th isotope data, version 1.00a. US Geological Survey Reston, VA, United States, 37 pp.

Ludwig, K.R. (2001): Isoplot/Ex – A Geochronological Toolkit for Microsoft Excel. Berkeley Geochronological Center Special Publication No. 1a, 43 pp.

Moev, M. and Antonov, M. (1978): Stratigraphy of the Upper Cretaceous in the eastern part of Strelcha – Chelopech line. *Ann. de l'École sup. mines et géol.*, **23**, Fasc. II Géol., 7–27 (in Bulgarian with English abstract).

Moritz, R., Jacquat, S., Chambefort, I., Fontignie, D., Petrunov, R., Georgieva, S., von Quadt, A. (2003): Controls on ore formation at the high-sulphidation Au–Cu Chelopech deposit, Bulgaria: evidence from infrared fluid inclusion microthermometry of enargite and isotope systematics of barite. In: Eliopoulos et al. (eds.): Mineral exploration and sustainable development, Millpress, Rotterdam, 1173–1176.

Müller, D., Rock, N.M.S. and Groves, D.I. (1992): Geochemical descrimination between shoshonitic and potassic volcanic rocks in different tectonic setting: a pilot study. *Mineral. Petrol.* **46**, 259–289.

Palmer, A. and Geissman, J. (1999): 1999 Geological time scale. *Geol. Soc. of America*, Product code CTS004.

Peytcheva, I. and von Quadt, A. (2004): The Palaeozoic protoliths of Central Srednogorie, Bulgaria: records in zircons from basement rocks and Cretaceous magmatites. Proceed. 5th Intern. Symp. on Eastern Mediterran. Geol., 14–20.04.2004, Thessaloniki, Greece, Vol. 1, 392–395.

Popov, P. and Kovachev, V. (1996): Geology, composition and genesis of the Mineralizations in the Central and Southern part of the Elatsite-Chelopech ore field. In: P. Popov (ed.): Plate Tectonic Aspects of the Alpine Metallogeny in the Carpato-Balkan region, UNESKO-IGCP Project No 356. Proccedings of the annual meeting, Sofia, 1, 159–170.

Popov, P., Petrunov, R., Strashimirov, S. and Kanazirski, M. (2000). Elatsite – Chelopech ore field. In: Guide to Excursions A and C of ABCD-GEODE 2000 Workshop, Sofia, 8–18.

Popov, P., Radichev, R. and Dimovski, S. (2002): Geology and evolution of the Elatzite-Chelopech porphyry-copper – massive sulfide ore field. *Ann. Univ. Mining and Geol.* **43–44/1**, 31–44.

Stacey, J.S. and Kramers, J.D. (1975): Approximation of terrestrial lead isotope evolution by a two-stage model. *Earth Planet. Sci. Lett.* **26**, 207–221.

Steiger, R.H. and Jäger, E. (1977): Subcommission on geochronology: Convention on the use of decay constants in geo- and cosmochronology. *Earth Planet. Sci. Lett.* **36**, 359–362.

Stoykov, S., Yanev, Y., Moritz, R. and Katona, I. (2002): Geological structure and petrology of the Late Cretaceous Chelopech volcano, Srednogorie magmatic zone. *Geochem. Mineral. Petrol.* **39**, 27–38.

Stoykov, S., Yanev, Y., Moritz, R. and Fontignie, D. (2003): Petrology, Sr and Nd isotope signature of the Late Cretaceous magmatism in the South-eastern part of Etropole Stara planina, Srednogorie magmatic zone. *Ann. Univ. Mining and Geol.* **46/1**, 201–207.

Stoykov, S. and Pavlishina, P. (2003): New data for Turonian age of the sedimentary and volcanic succession in the southeastern part of Etropole Stara Planina Mountain, Bulgaria. *C. R. Acad. bulg. Sci.* **56/6**, 55–60.

Strashimiriov, S., Ptrunov, R. and Kanazirski, M. (2002): Porphyry-copper mineralization in the central Srednogorie zone. *Mineralium Deposita* **37**, 587–598.

Velichkova, S., Handler, R., Neubauer, F. and Ivanov, J. (2001): Preliminary $^{40}Ar/^{39}Ar$ mineral ages from the Central Srednogorie Zone, Bulgaria: Implication for the Cretaceous geodynamics. In: ABCD GEODE workshop, Vata Bai, *Romanian Journal of Mineral deposits* **79/ 2**, 112–113.

Voldet, P. (1993): From neutron activation to inductively coupled plasma-atomic emission spectrometry in the determination of rare-earth elements in rocks. *Trends in Analytical Chemistry* **12**, 8–15.

von Quadt, A., Ivanov, J. and Peytcheva, I. (2001): The Central Srednogorie (Bulgaria) part of the Cu (Au–Mo) belt of Europe: A review of the geochronological models in the light of the new structural and isotopic studies. In: Piestrzyski, L.A. (ed.): Mineral deposits at the Beginning of the 21st Century. Swets & Zeitlinger Publishers, Lisse, 555–558.

von Quadt A., Peytcheva, I., Kamenov, B., Fanger, L., Heinrich, C.A. and Frank, M. (2002): The Elatsite porphyry copper deposit in the Panagyurishte ore district, Srednogorie zone, Bulgaria: U–Pb zircon geochronology and isotope-geochemical investigations of magmatism and ore genesis. In: Blundell, D.J., Neubauer, F. and von Quadt, A. (eds.): The Timing and Location of Major Ore Deposits in an Evolving Orogen. *Geol. Soc. London Spec. Publ.* **204**, 119–135.

von Quadt, A., Peytcheva, I. and Cvetkovic, V. (2003): Geochronology, geochemistry and isotope tracing of the Cretaceous magmatism of East-Serbia and Panagyurishte district (Bulgaria) as part of the Apuseni-Timok-Srednogorie metallogenic belt in Eastern Europe. In: Eliopoulos, D.G. et al. (eds.): Mineral Exploration and Sustainable Development, Millpress, Rotterdam, **1**, 407–410.

Zimmerman, A., Stein, H., Markey, R., Fanger, L., Heinrich, C., von Quadt, A. and Peytcheva, I. (2003): Re–Os ages for the Elatsite Cu–Au deposit, Srednogorie zone, Bulgaria. In: Eliopoulos et al. (eds), Mineral exploration and sustainable development, Millpress, Rotterdam, 1253–1256.

Zindler, A. and Hart, S.R. (1986): Chemical geodynamics. *Ann. Rev. Earth Planet. Sci.* **14**, 493–571.

Received 26 January 2004
Accepted in revised form 30 August 2004
Editorial handling: T. Driesner